**Title**
OBSERVATION OF INTERFERENCE EFFECTS IN THE REACTION n+p->n+pno



**Author**
Michael, W.

**Publication Date**
1972-10-01

LBL-1024
Preprint c.1

# OBSERVATION OF INTERFERENCE EFFECTS IN THE REACTION $\pi^+p \rightarrow \pi^+p\pi^o$

W. Michael

October 1972

AEC Contract No. W-7405-eng-48

LBL-1024

# Observation of Interference Effects in the Reaction $\pi^+ p \rightarrow \pi^+ p \pi^0$*

W. Michael
E. O. Lawrence Berkeley Laboratory
University of California
Berkeley, California 94720

## Abstract

In the reaction $\pi^+ p \rightarrow \pi^+ p \pi^0$ at 2.67 GeV/c, the central value of the $\rho$ mass peak and its width are found to vary as a function of position in the Dalitz plot. The major variations are associated with the cross-over regions of $\rho p$ with diffractively produced $\pi^+(p\pi^0)$ and $\pi^+ N^*$ final states, and so have a natural interpretation in terms of interferences among these final states.

* Work done under the auspices of the U.S. Atomic Energy Commission.

In a study of $\rho^+$ production in the reaction

$$\pi^+ p \rightarrow \pi^+ p \pi^0 \qquad (1)$$

at 2.67 GeV/c, the central value of the $\rho$ mass peak and its width are found to vary as a function of position in the Dalitz plot.[1] These variations are associated with the cross-over regions of the $\rho p$ final state with $\Delta\pi$, $N^*\pi$, and diffractively produced $\pi^+(p\pi^0)$ states, and so have a possible interpretation in terms of interferences among these final states. Such an interference of $\rho p$ with diffractive dissocation of the proton has been suggested by J. MacNaughton et al.,[2] as a means of accounting for a mass-dependent asymmetry in the di-pion t-channel helicity (or Gottfried-Jackson) angular distribution, or, alternatively, a shift in the $\rho$ mass as a function of this angle. Such effects have long been studied in terms of $\pi\pi$ scattering phase shifts, where this behavior is attributed to interference of an S-wave, I = 2 amplitude with the resonant P-wave I = 1 state.[3,4] However, since the known exchanges in $\rho$ production include, in addition to the pion quantum numbers, both isoscalar and isovector, natural and unnatural parity, non-zero spin states,[1,3] and since the changes in apparent mass and width reported here are associated with the cross-over in the Dalitz plot of $\rho p$ and $\pi N^*$ states, it appears desirable to consider an interpretation in the context of the overall $\pi^+ p \pi^0$ production reaction. The analysis of Reference 2 falls in this category. Those authors emphasize that their interpretation may well be equivalent to the OPE approach at the pion pole, and hence does not necessarily invalidate the determination of $\pi\pi$ phase shifts, provided the extrapolations involved are from a region of small enough momentum transfer. On the other hand, their model (to be discussed in more detail below) accounts in a natural way for some of the more striking features of the data to be reported here, features which are not adequately described by the known $\pi\pi$ scattering phase shifts.[2,3,4]

The present analysis is based on some 8400 events of reaction (1), obtained from a 300,000 picture exposure of the 25" hydrogen bubble chamber to a $\pi^+$ beam of 2.67 GeV/c momentum.[1] The Dalitz plot of these events, given in Fig. 1, shows that the dominant processes are the quasi-two-body production of $\rho p$ and $\Delta^{++}(1236)\pi^o$. Also apparent in the $\pi^o p$ Chew-Low plot and mass-squared projection, Fig. 2, are small amounts of higher mass $N^*$'s, and a broad distribution in mass from threshold to about 1700 MeV, produced at small momentum transfer. This latter distribution is identified as diffractive dissociation of the proton.[2,5]

Inspection of Fig. 1 gives a qualitative indication of the variation of the apparent mass and width of the $\rho$ as a function of the ordinate of the plot. To quantify this observation, the plot has been divided into six segments (indicated by the horizontal lines in Fig. 1), and a maximum-likelihood fit of the apparent resonance parameters of the $\rho$ has been made for each segment.[6] A description of the fitting procedure is given in Appendix Ia. The results of these fits are given in Table Ia, along with a list of the major crossing baryon states in each segment. The variation in apparent mass across the plot is seen to be about 60 MeV, with the greatest change associated with segment six. There is also a variation in the apparent width, with the greatest changes associated with segments four and five. The possibility that these variations result from experimental biases has been excluded in the manner described in Appendix II.

Further evidence of the nature of the effects observed here is given in Fig. 3, which shows the distribution of the di-pion t-channel helicity cosine, $\cos\theta^t_{\pi\pi}$, for four slices of di-pion mass. There is evidently present some effect which causes a depletion in the forward direction for di-pion masses below the $\rho$ mass (Fig. 3a), changes sign with increasing mass, and leads to an enhancement in the forward direction for di-pion masses above the $\rho$ mass (Figs. 3c and 3d). This behavior suggests an interference between different processes leading to the di-pion final state.

The association of this effect with diffractive dissociation of the proton is demonstrated in Fig. 4, where histograms are shown of the di-pion mass for six intervals of $\cos\theta^t_{\pi\pi}$. For these distributions, a cut has been applied to the four-momentum transfer from beam to di-pion, $-t_p$, selecting events in the forward peak of the $\rho$ production differential cross section, in order to limit the $\rho$ production amplitude to a more well-defined phase, and thus better isolate effects depending on this phase. (This is also the region in which pion exchange is most important.) The cut has been made at $-t_p = 0.3$ $(GeV/c)^2$, just below the first dip in the differential cross section.[1] The scatter plot in Fig. 4 shows the close relationship in the forward direction between $\cos\theta^t_{\pi\pi}$ and the four-momentum transfer from beam to outgoing $\pi^+$, $-t_\pi$ (for which the Chew-Low plot is shown in Fig. 2). Thus a selection of the forward interval of $\cos\theta^t_{\pi\pi}$ also selects events of low $-t_\pi$, that is, events of diffractive dissociation of the proton. Fig. 4f shows the very pronounced change in central value and shape of the $\rho$ peak associated with this selection.

To measure the shifts in the central value of the peak, the distributions of Fig. 4 have been fitted as described in Appendix Ib. The results of these fits for the intervals of $\cos\theta^t_{\pi\pi}$ are given in Table Ib. In the forward interval (Fig. 4f), the peak of the distribution is shifted by about 60 MeV from the accepted value for the $\rho$ mass. The shape of the distribution is skewed, showing a very steep slope and depletion of events on the low-mass side, and a more gradual slope on the high-mass side. Both the shift and the skewing may be understood in terms of an interference that is destructive below the $\rho$ mass and constructive above it. For intervals of decreasing value of $\cos\theta^t_{\pi\pi}$ (Fig. 4e-4b), the central value of the peak decreases and the skewing tends to change sign. In interval (a) (Fig. 4a), the peak value is 765 ± 6 MeV, which agrees well with the accepted value for the $\rho$ mass. Interval (a) is the only one in which the $\rho$ is not the dominant signal, with production of $\Delta^{++}(1236)$ accounting for more than one-half the events in that interval.

The suggestion of Reference 2 is that the distributions of di-pion mass be represented by an amplitude of the form

$$A_{\pi\pi} = A_\rho + A_d \qquad (2)$$

where the $\rho$ amplitude is approximated by

$$A_\rho \propto \frac{a \cos\theta^t_{\pi\pi}}{(m_\rho^2 - m_{\pi\pi}^2) - i\, m_\rho \Gamma} \qquad (3a)$$

and the diffractive amplitude by

$$A_d \propto e^{i\delta}\, e^{(\gamma/2)t\pi} \qquad (3b)$$

where $m_{\pi\pi}$ is the di-pion mass, $m_\rho$ and $\Gamma$ are the $\rho$ mass and width taken to be 765 and 165 MeV respectively, and a is related to the density matrix, $\rho_{ij}$, of the $\rho$, and is taken to be $\sqrt{\rho_{00}} \simeq 0.8.$[1] $\delta$ is a phase to be adjusted by fitting the data, and $\gamma$ is an average slope for the angular distribution of the diffractive process, taken from the data to be 4 $(\mathrm{GeV}/c)^{-2}$. This form of the amplitude has been fitted to the forward interval (Fig. 4f), using the maximum likelihood approach described in Appendix I (with appropriate replacement of the form of the distribution), and the angle $\delta$ is found to be 172 ± 10 degrees, in excellent agreement with the value 170 ± 6 degrees found in Reference 2. Some simple refinements of the above model can be immediately suggested, for example, the amplitude $A_\rho$ (eq. 3a) could contain a factor $e^{(\epsilon/2)t_p}$, where $\epsilon$ is taken from the $\rho$ production differential cross section in the t-range considered; the azimuthal terms of the $\rho$ decay angular distribution could be included; and possible additional interferences with the $N^*$'s could be considered, particularly for describing the full angular ranges of di-pion production and decay. The development of such a detailed model is, however, outside the scope of this report.

In summary, the data presented here demonstrate the presence of effects in the di-pion mass spectrum that can best be described as resulting from interferences among competing processes leading to the $\pi^+ p\, \pi^0$ final state. At small momentum transfer, interference between $\rho$ production and diffractive dissociation of the proton causes a pronounced shift and skewing of the $\rho$ mass peak. Variations in the width are also observed, with the greatest variations associated with the cross-over of the $\rho p$ state with $\pi N^*(1688)$ and $\pi N^*(1500)$.

It is my pleasure to thank Mr. Fred Lott for several invaluable discussions, and Dr. George Gidal, Dr. Robert Ely, and Dr. Robert Birge for many things.

## Appendix I

a) The parameters given in Table Ia were determined assuming no coherence among the contributing processes. Each segment of the Dalitz plot was fitted with a distribution, D, of the form $D = \Sigma b_k + \Phi$, where $b_k$ is a Breit-Wigner line shape convoluted with a triangular resolution function (see Appendix II and Refs. 7, 8). A P-wave shape was used for the $\rho$ and $\Delta(1236)$ resonances, and an S-wave shape for the higher, less well resolved $N^*$'s. $\Phi$ represents a constant phase-space-like background. The proton diffractive dissociation process was not explicitly parameterized. A check of the quality of the fits was made by computing the $\chi^2$ of the experimental mass-squared histograms to the projected distributions obtained with the fitted parameters. The average $\chi^2$ per degree of freedom is 1.6.

b) The parameters given in Table Ib were determined as described in a) above except that the expression for D contains only terms for $\rho$, $\Delta(1236)$, and $\Phi$, since with the cuts applied no other resonance signals are statistically significant.

## Appendix II

The possibility that significant mass shifts were introduced by the kinematic fitting procedure has been ruled out by repeating the appropriate histograms using the unfitted di-pion mass. The distributions in unfitted mass (not shown) show the same effects displayed in Figs. 1, 3, and 4.

The apparent width of the peak depends on the resolution of the di-pion mass-squared. To account for this, the Breit-Wigner functions used in the fit have been convoluted with a triangular resolution function,[8] and for each event the calculated error on the di-pion mass-squared is used in calculating the weight of that event. Thus, the widths quoted in Table I represent "true" widths within the limitations inherent in the model. The overall correctness of these error assignments has been checked in two ways. First, the experimental distribution of $\chi^2$ for the kinematic fit of the events in the data sample is found to have a mean value of 0.83, where 1.0 is expected. Secondly, since the missing mass-squared to the proton and its error are the quantities of interest, it is desirable to examine a system in which this missing mass is a $\delta$-function, and to compare the calculated resolution width with the width of the experimentally observed distribution. This has been done using a sample of elastic scattering events from the same film. The elastic events (identified by a four-constraint fit) were re-fitted using one constraint only, ignoring the outgoing $\pi^+$ momentum vector. The resolution width computed from the most probable error for these events is 0.047 $GeV^2$, while the width of the observed distribution of missing mass-squared is found to be 0.042 $GeV^2$.

## References

1. W. Michael and G. Gidal, Physical Review Letters 28, 1475 (1972).
2. J. MacNaughton, W. R. Butler, D. G. Coyne, C. Fu, and G. H. Trilling, UCRL-20833 (unpublished).
3. J. P. Baton, et. al., Physics Letters 33B, 528 (1970).
4. P. E. Schlein, Lecture Notes for the International School of Subnuclear Physics, Erice, Sicily (1970).
5. K. Boesebeck, et. al., Nuclear Physics B28, 381 (1971).
6. The maximization was done with the program OPTIME by Philippe Eberhard and Werner O. Koellner, UCRL-20159, 20160.
7. J. D. Jackson, Nuovo Cimento 34, 1644 (1964).
8. D. G. Coyne, et. al., Nuclear Physics B32, 333 (1971).

Table I. Apparent mass and width of the $\rho$ resonance: a) in the segments of the Dalitz plot defined in Fig. 1, and b) in the intervals of $\cos\theta^t_{\pi\pi}$ defined in Fig. 4. The errors quoted reflect only the statistical uncertainties.

| (a) Segment of Dalitz plot (see Fig. 1) | Mass (MeV) | Width (MeV) | Major crossing states | (b) Interval of $\cos\theta^t_{\pi\pi}$ (see Fig. 4) | Mass (MeV) | Width (MeV) |
|---|---|---|---|---|---|---|
| 1 | 764 ± 5 | 127 ± 15 | $\Delta^{++}$(1236) | a | 765 ± 6 | 119 ± 17 |
| 2 | 754 ± 6 | 172 ± 20 | -- | b | 724 ± 8 | 148 ± 25 |
| 3 | 753 ± 8 | 204 ± 27 | -- | c | 732 ± 5 | 124 ± 16 |
| 4 | 776 ± 9 | 237 ± 35 | N(1688),dd[a] | d | 750 ± 7 | 169 ± 24 |
| 5 | 792 ± 10 | 247 ± 40 | N(1500),dd[a] | e | 790 ± 7 | 170 ± 21 |
| 6. | 816 ± 6 | 168 ± 20 | $\Delta^{+}$(1236),dd[a] | f | 823 ± 5 | 165 ± 16 |

[a] "dd" denotes diffractive dissociation of the proton.

## Figure Captions

Fig. 1. Dalitz plot of the reaction $\pi^+p \rightarrow \pi^+p\ \pi^0$ at 2.67 GeV/c. The histograms 1) - 6) show the di-pion mass projection of the correspondingly labeled segment of the Dalitz plot. The segment boundaries are at -2.50, -1.25, 0., 1.25, and 2.50 GeV$^2$. The dash-dot line in the histograms is at 770 MeV.

Fig. 2. Chew-Low plot and mass-squared projection for the $\pi^0p$ system.

Fig. 3. t-channel helicity cosine distribution of the di-pion, $\cos\theta^t_{\pi\pi}$, for four intervals of di-pion mass-squared.

Fig. 4. Di-pion mass distributions in six intervals of $\cos\theta^t_{\pi\pi}$, with the four-momentum transfer to the di-pion less than 0.3 (GeV/c)$^2$. The interval boundaries are at -0.7. -0.4, 0., 0.4, and 0.7. The dash-dot line in the histograms is at 770 MeV.

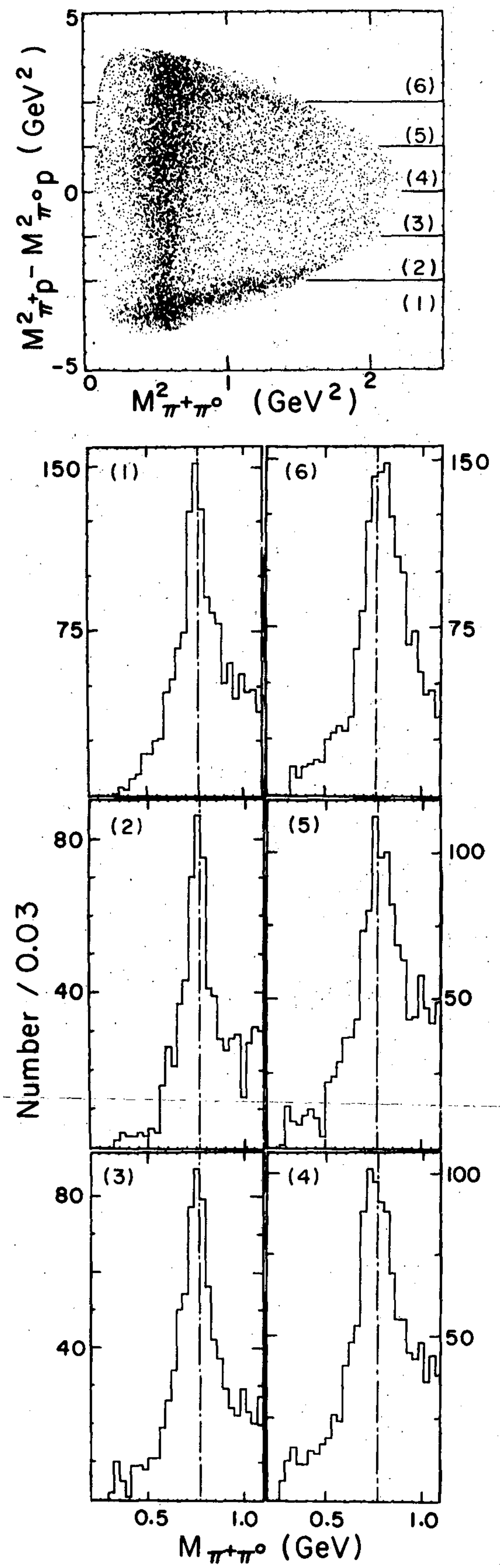


XBL726-3139

Fig. 1

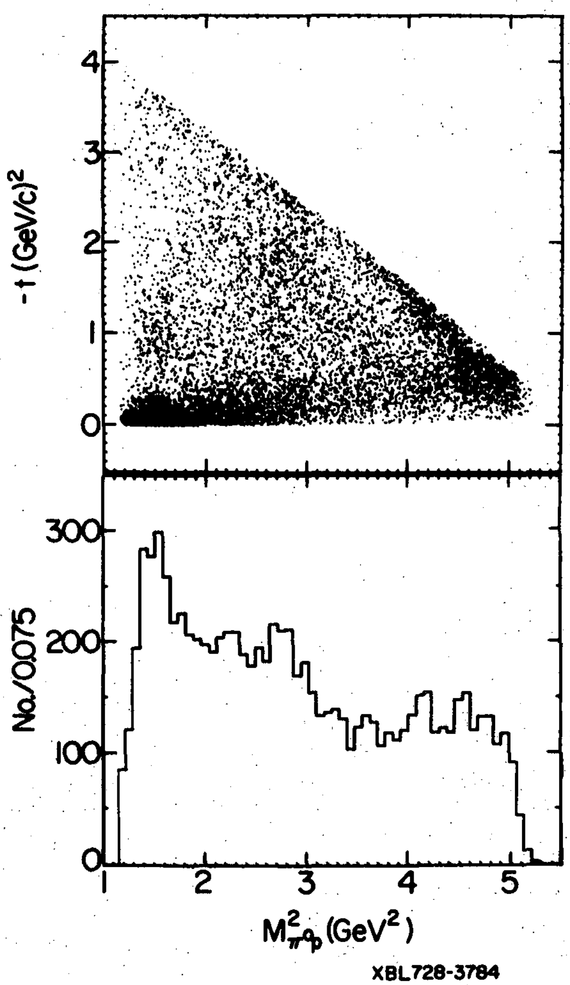
-t (GeV/c)$^2$
4
3
2
1
0
300
200
100
0
No./0.075
1
2
3
4
5
$M^2_{\pi^0 p}$ (GeV$^2$)
XBL728-3784

Fig. 2

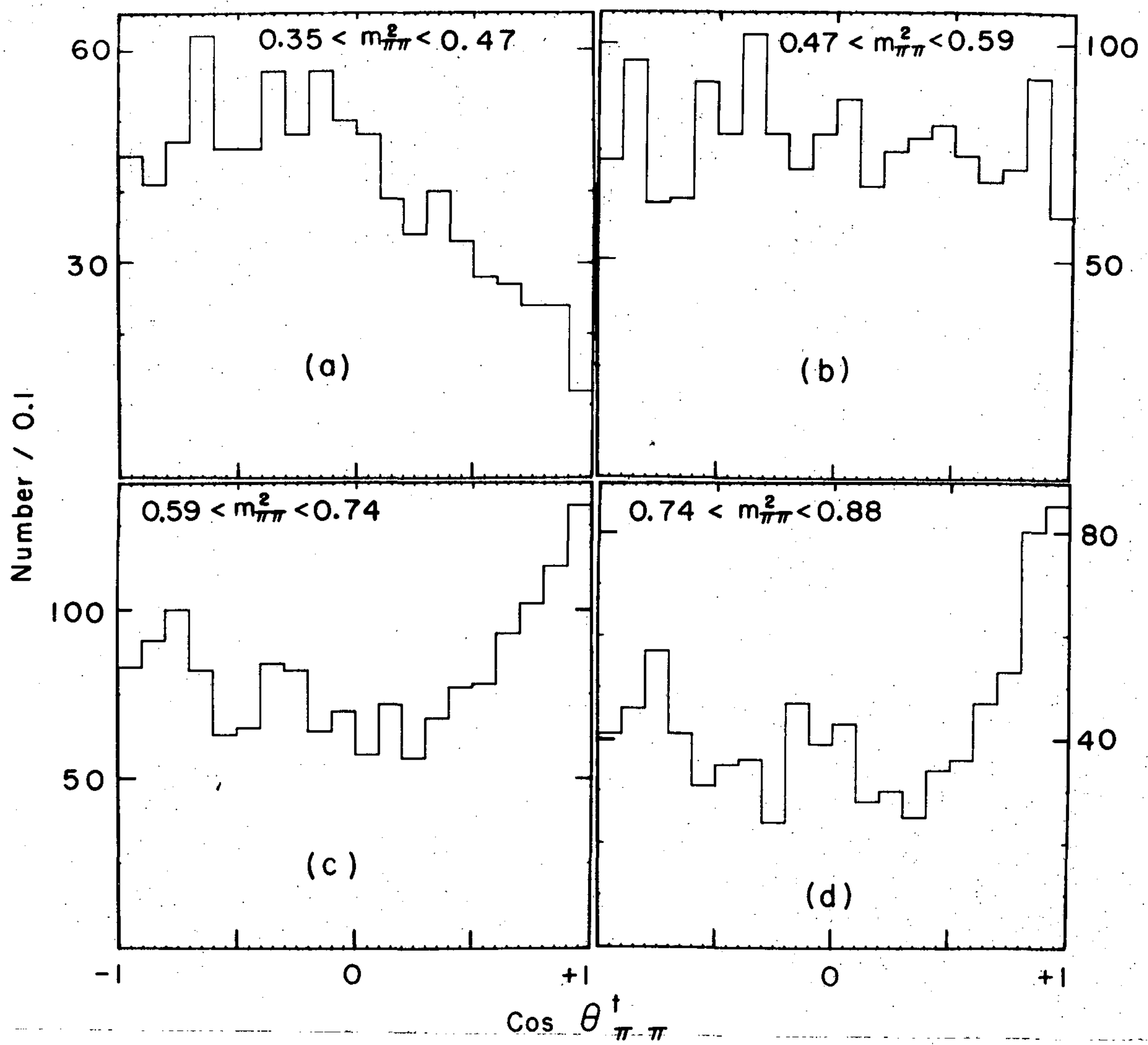


XBL725-3093

Fig. 3

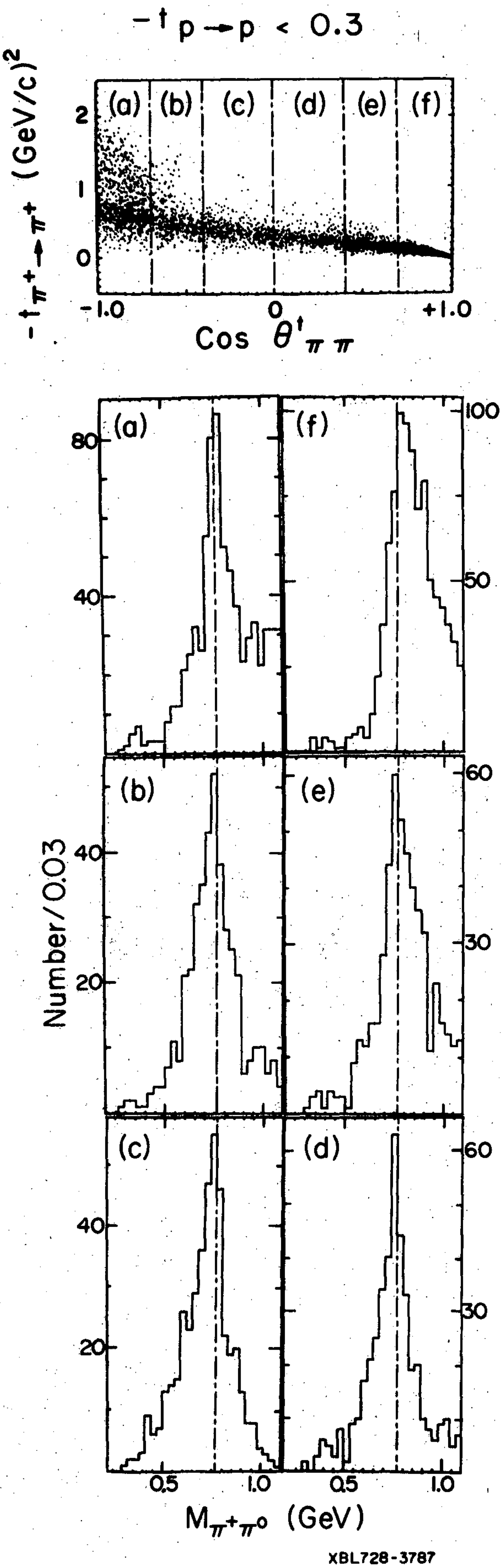

$-t_{p\to p} < 0.3$
$-t_{\pi^+\to\pi^+}$ (GeV/c)$^2$
(a) (b) (c) (d) (e) (f)
2
1
0
-1.0
0
+1.0
Cos $\theta'_{\pi\pi}$
(a)
(b)
(c)
(d)
(e)
(f)
80
40
40
20
40
20
100
50
60
30
60
30
Number/0.03
0.5
1.0
0.5
1.0
$M_{\pi^+\pi^0}$ (GeV)
XBL728-3787


Fig. 4

TECHNICAL INFORMATION DIVISION
LAWRENCE BERKELEY LABORATORY
UNIVERSITY OF CALIFORNIA
BERKELEY, CALIFORNIA 94720